Eu^{3+} luminescence: A spectral probe in $M_5(PO_4)_3X$ apatites (M=Ca or Sr; $X=F^-$, Cl^-, Br^- or OH^-)

1995 J. Phys.: Condens. Matter 7 8453

(http://iopscience.iop.org/0953-8984/7/44/014)

J. Phys.: Condens Matter 7 (1995) 8453–8466. Printed in the UK

Eu^{3+} luminescence: a spectral probe in $M_5(PO_4)_3X$ apatites (M = Ca or Sr; X = F^-, Cl^-, Br^- or OH^-)

R Jagannathan and M Kottaisamy

Central Electrochemical Research Institute, Karaikudi-623006, India

Received 28 November 1994, in final form 19 July 1995

Abstract. Eu^{3+} luminescence is of special importance as a spectral probe apart from its application in phosphor materials. This is possible for the reason that Eu^{3+} has several structure-dependent transitions enabling one to gain insight about the site that it occupies in a given host. On this basis we have attempted to explore the different cationic sites present in the apatite system. In fluoroapatites, Eu^{3+} predominantly occupies M_{II} sites, with the local symmetry becoming enhanced from C_{1h} to a tetragonal symmetry attributed to charge-compensating species. In addition to both kinds of site of the apatite system (M_I and M_{II}) occupied by Eu^{3+}, we have observed the presence of a third kind of Eu^{3+} site. The observation of unusually strong $^5D_0 \rightarrow {}^7F_0$ emission of Eu^{3+} in fluoroapatites and bromoapatites has been explained. Also various results on the luminescence features of Eu^{3+} correlated with the structural details known are discussed.

1. Introduction

The $M_5(PO_4)_3X$ (M = alkaline earths; X = F^-, Cl^-, Br^- or OH^-) type of apatite materials have been extensively studied for their technological importance, especially fluoroapatites and chloroapatites as phosphor materials and laser hosts [1, 2] and hydroxyapatites as biocompatible materials [3]. The crystallography of these apatites is well documented in literature [4, 5]. Also, there are some reports using Eu^{3+} luminescence as a tool to probe the local microscopic symmetry of the site(s) that it occupies in the apatite system [6–8], but unique agreement between them seems to be impossible. Furthermore, we observe that the results obtained in this investigation are very different from those described recently by Zounani *et al* [8] on Eu^{3+} luminescence in strontium fluoropatite (SFAP), in particular with regard to firstly the site occupancy by Eu^{3+} ions and (secondly) the occurrence of $^5D_0 \rightarrow {}^7F_0$ emission in fluoroapatite.

Also, as far as we are aware, no reports are available concerning the Eu^{3+} luminescence in hydroxyapatite and bromoapatite systems. Hence we thought it worthwhile to investigate the apatite system in a more detailed way using Eu^{3+} luminescence as a spectral probe. The advantages of using Eu^{3+} luminescence as a spectral probe are as follows.

(i) Trivalent europium has a relatively simple electronic energy level scheme.

(ii) The non-degenerate $^5D_0 \rightarrow {}^7F_0$ transition will clearly indicate the presence of multiple cationic sites present in the host.

(iii) Some of the transitions, in particular $^5D_0 \rightarrow {}^7F_2$, are hypersensitive to the chemical surroundings and are symmetry dependent, as these are expected to be absent in centrosymmetric sites.

0953-8984/95/448453+14$19.50

Another salient feature of this investigation is the occurrence of an intense $^5D_0 \rightarrow {}^7F_0$ transition in fluoroapatites and bromoapatites, which is forbidden by the angular momentum selection rule ($J = 0 \not\rightarrow J = 0$). Interestingly the same transition is absent in isomorphous hydroxyapatites and chloroapatites. Using Eu^{3+} luminescence as a probe, various results obtained on these apatites are discussed.

2. Experimental details

The preparation of fluoroapatites, chloroapatites and bromoapatites involves the solid state reaction between the various reactants taken in suitable proportion to satisfy the following equations:

$$6MHPO_4 + 3Ca_{1-x}CO_3(/4Sr_{1-x}/(4Ba_{1-x})CO_3) + CaF_2(/2NH_4F/2NH_4Br) + xEu_2O_3 \rightarrow 2M_{5-x}Eu_x(PO_4)_3X + (\text{gases} + H_2O) \quad (1)$$

for M = Ca, Sr or Ba and X = F^- or Br^-;

$$6MHPO_4 + 4Ca_{1-x}CO_3(3SrCO_3) + 2NH_4Cl/SrCl_2 \cdot 6H_2O + xEu_2O_3 \rightarrow 2M_{5-x}Eu_x(PO_4)_3Cl + (\text{gases} + H_2O) \qquad \text{for M = Ca and Sr.} \quad (2)$$

In these apatites, 0.5–5 mol% Eu was added as Eu_2O_3 in the above reaction(s) such that the europium concentration is also taken into consideration for calculating the metal($M^{2+} + Eu^{3+}$)-to-phosphorus (P) ratio. It should be noted that, according to the above equation(s), the theoretical ratio should be 5 to 3, but in actual practice the best results (in terms of luminous intensity) are obtained only for cases where the metal(including Eu^{3+})-to-P ratio is in the range 4.9–4.95 to 3. The various reactants taken in the above ratio are thoroughly homogenized in an agate mortar and transferred to an alumina crucible. Then it is charged into a resistance-heated furnace kept at 1100 °C for 2 h. The firing atmosphere used is open air to maintain europium in its trivalent state and we have also found that there is no trace of divalent europium as evidenced from the absence of band emission characterizing the $4f^65d \rightarrow {}^8S$ transition normally found in this host. In order to compensate for the volatalization losses of the halides used in the preparation, an addition of 10% excess halides was found to yield the required apatite phase. All these firings are done with crucibles covered with suitable lids. After this they are air quenched. Then the products obtained are checked for their phase content and purity using the x-ray powder pattern technique. The phases obtained matched quite well the standard JCPDS files and then these samples are used for luminescence measurements. For the preparation of hydroxyapatites we refer to the standard procedure given by Butler [1]. In particular, the calcium hydroxyapatite (CHAP) doped with trivalent europium studied in this investigation was prepared as given below. The required amount of calcium nitrate dissolved in 300 ml of freshly boiled deionized water (free of dissolved carbon dioxide) was added to 7.3 ml of europium nitrate solution (corresponding to 5 mol% Eu^{3+}) and maintained at 90 °C. Then dilute liquid ammonia was added until the pH reached 8. 2.04 g of di-ammonium hydrogen orthophosphate dissolved in 200 ml of water was added dropwise to the above solution with constant stirring using a Teflon-coated stirrer. Then the precipitate was digested for 6 h and washed thoroughly to be free of unreacted components. Then the precipitate was filtered and oven dried at 110 °C. After this it was sintered at 950 °C for 2 h in an open-air atmosphere. The x-ray powder pattern of the product thus obtained matched quite well the standard patterns corresponding to CHAP available in the JCPDS files. The oven-dried CHAP: Eu^{3+} (found to be x-ray amorphous) was also used for luminescence measurements. All the luminescence spectral recordings (both emission and excitation spectra) were recorded

using a Hitachi 650-10S fluorescence spectrophotometer (employing a stigmatic concave diffraction grating and with an F/aperture number of 3). This system is equipped with a 150 W xenon arc discharge lamp and Hamamatsu R928F photomultiplier tube as the excitation source and detector, respectively. The excitation spectra obtained were corrected for the beam intensity variation of the light source used. The spectral recordings were done at both room temperature and liquid-air temperature ($T = 300$ K and 100 K, respectively). The other experimental procedures were the same as described earlier [9].

3. Results and discussion

3.1. Structural aspects of apatites

$M_5(PO_4)_3X$ (M = alkaline earths; X^- = F^-, Cl^-, Br^- or OH^-) apatites crystallize in a hexagonal or pseudo-hexagonal system. In the apatite family the fluoroapatite has the highest symmetry with the space group corresponding to $P6_3/m$ which can be attributed to the occurrence of fluoride ions in the planes of triangles constituted by alkaline earths. For larger X^- ions (X^- = Cl^-, Br^- or OH^-) this system crystallizes in an isomorphous pyromorphite-type lattice for which the space group symmetry is lowered to $P6_3$ (the glide mirror plane perpendicular to the c axis is lost) [5]. This is because the larger X-ions take the positions along the c direction that intersect the plane(s) of triangles constituted by the alkaline earths.

In the apatite structure there are two types of cationic site (M_I and M_{II}) with their relative abundances being in the ratio 4:6. The first type of site (M_I) has trigonal symmetry (C_3) due to the tricapped trigonal prism formed by nine oxygen atoms surrounding the cationic site. The second type of site is seven coordinated with six oxygen atoms and one X^- ion with the local symmetry that can be described by the C_{1h} (C_s) point group. These two site symmetries can be pictorially represented as in figure 1. The second type of cation creates an open channel along the z direction parallel to the c axis. The oppositely oriented triangular planes connecting M_{II} ions occur at positions $z = 1/4, 3/4$. The position of X^- ion(s) along the channel is decided by its size and charge, leading to a change in crystallographic symmetries for various apatites. It should be noted that, in the case of fluoroapatites, the fluoride ion(s) occur in the plane of triangles while in the case of larger halogens or hydroxyl ions they occur out of the plane(s) of the triangles as depicted in figure 1.

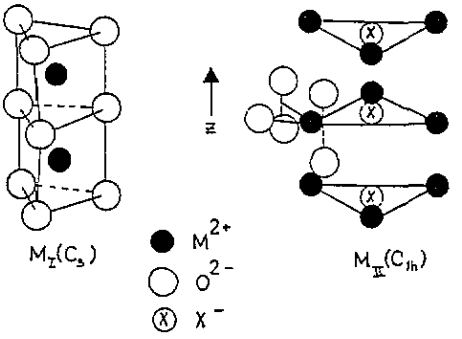

Figure 1. Schematic representation of two types of cationic site (M_I and M_{II}) possible in $M_5(PO_4)_3X$ apatites (where M^{2+} = Ca^{2+} or Sr^{2+}; X^- = F^-, Cl^-, Br^- or OH^-).

3.2. Some general principles of Eu^{3+} luminescence spectroscopy

Trivalent europium having a $4f^6$ configuration in a number of host matrices leads to intense orange–red emission (590–625 nm) due to various $^5D_0 \rightarrow {}^7F_J$, $J = 0, 1$–4 (especially $J = 1$ and 2) transitions. These intraconfigurational transitions are parity forbidden by Laporte selections rules [10] and are expected to be absent when occupying centrosymmetric crystallographic sites of a crystal lattice. Notably, the hypersensitive $^5D_0 \rightarrow {}^7F_2$ electric dipole transition is expected to be absent in centrosymmetric site(s). Nevertheless this transition can be observed even in centrosymmetric sites as a weak red emission which can be attributed to the mixing of odd terms due to the crystal field.

Another interesting feature of the Eu^{3+} luminescence is that its relatively simple energy level structure, especially ^7F_J, enables one to ascertain the microscopic symmetry around the site. This is possible by finding the number of Stark components for a given transition. The Stark components for various $^5D_0 \rightarrow {}^7F_J$ ($J = 0, 1$ and 2) levels under different point-group symmetries possible in the apatite system are given in table 1 [11]. Furthermore, the non-degenerate $^5D_0 \rightarrow {}^7F_0$ emission line acquires special importance in that it will reveal the presence of crystallographic inequivalent sites in a given host matrix. These can be easily studied with the help of site-selective spectroscopy by addressing the excitation to a particular site or level. With regard to site-selective excitation, it is necessary that one should be able to pick up a particular excitation level, which becomes difficult unless these are excited by tunable lasers. For this reason the Eu^{3+}–O^{2-} charge-transfer excitation band (about 250–300 nm) and other intense excitation lines, namely $^7F_0 \rightarrow {}^5L_6$ (about 395 nm) and $^7F_0 \rightarrow {}^5D_2$ (about 465 nm), turn out to be non-selective excitations.

Another important point that should be borne in mind is that high-frequency vibrations of the phosphate lattice ($\omega_{max} = 1200\ cm^{-1}$) will enhance the $^5D_1 \rightarrow {}^5D_0$ relaxation process. This will leave less scope for the $^5D_1$ level of Eu^{3+} to be the emitting level in this system. Hence for all practical purposes the emitting level will be solely $^5D_0$, the non-degenerate level. Also, in the present paper, the emission transitions $^5D_0 \rightarrow {}^7F_3$ and $^5D_0 \rightarrow {}^7F_4$ are not presented because firstly the former emission is very weak and secondly with the moderate spectral resolution it is difficult to study transitions to higher J-values. Also we find that, in the emission spectra recorded for the different apatite host matrices, a narrow band emission characteristic of the $4f^65d \rightarrow {}^8S_{7/2}$ transition of Eu^{2+} is not observable. This indicates the absence of Eu^{2+} luminescent centres.

3.3. Eu^{3+} luminescence in fluoroapatites

Emission spectra of Eu^{3+} in calcium fluoroapatite (CFAP) and strontium fluoroapatite (SFAP) under both selective and non-selective excitations are given in figures 2 and 3.

3.3.1. Calcium fluoroapatite: Eu^{3+}. For the non-selective excitation corresponding to the $^7F_0 \rightarrow {}^5L_6$ transition (at 395 nm), one can observe a complex emission spectrum as in figure 2. The presence of intense line emission at 576 nm corresponding to the $^5D_0 \rightarrow {}^7F_0$ transition of Eu^{3+} occupying a particular site is an interesting situation.

For the selective excitation (at either 572 or 576 nm) corresponding to the two types of $^5D_0 \rightarrow {}^7F_0$ level of Eu^{3+}, one can see that different $^5D_0 \rightarrow {}^7F_2$ components appear with better clarity than for non-selective excitation. It has been found in the present investigation that, for the various apatites ($X^- = F^-$, Cl^-, Br^- or OH^-) studied, the occurrence of the intense $^5D_0 \rightarrow {}^7F_0$ line emission is mainly dependent on the type of apatite in which Eu^{3+} is present. Hence, this suggests that this intense $^5D_0 \rightarrow {}^7F_0$ line corresponds to Eu^{3+}

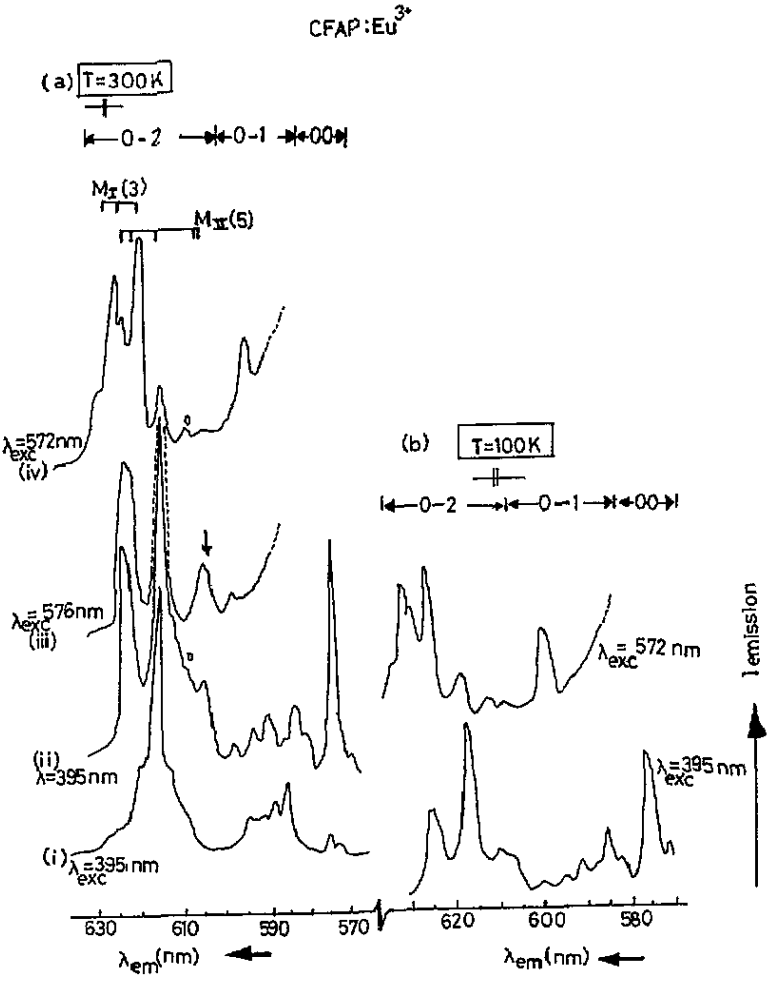

Figure 2. Eu^{3+} emission sprectra for CFAP at (a) 300 K and (b) 100 K under different excitation conditions: $M_{II}(5)$, the $^5D_0 \rightarrow {}^7F_2$ emission (five Stark components) of the predominant $Eu^{3+}(M_{II})$ sites; $M_I(3)$, the $^5D_0 \rightarrow {}^7F_2$ emission (three Stark components) of the less dominant $Eu^{3+}(M_I)$ sites; O, emission components of the third kind of (distorted) Eu^{3+} site; 0–0, 0–1, and 0–2, $^5D_0 \rightarrow {}^7F_J$ ($J = 0$, 1 and 2, respectively) emission lines of Eu^{3+}. In (a) the emission spectra of Eu^{3+} in CFAP are for the following Eu^{3+} concentrations: curve (i), 0.5 mol%; curves (ii)–(iv), 5 mol%.

occupying the second kind (M_{II}) of cationic site of the apatite system, in which the cation is coordinated to the X^- ion in addition to six oxygen atoms of the $(PO_4)^{3-}$ group. The site symmetry corresponding to the second kind of site (M_{II}) in apatites is Cs (C_{1h}). This predicts five Stark components for the $^7F_2$ level. On selective excitation at 576 nm, one can observe five Stark components at 16 012 cm^{-1}, 16 048 cm^{-1}, 16 247 cm^{-1}, 16 474 cm^{-1} and 16 515 cm^{-1} (624.5 nm, 623.1 nm, 615.5 nm, 607 nm and 605.5 nm respectively (table 2 and figure 2(a)) for the $^5D_0 \rightarrow {}^7F_2$ emission. However, for this emission except for the central component the other components are not well resolved to account for the remaining four Stark levels to be consistent with C_{1h} site symmetry. It is apparent that the charge-compensating species (for the trivalent europium occupying the divalent cationic site) may

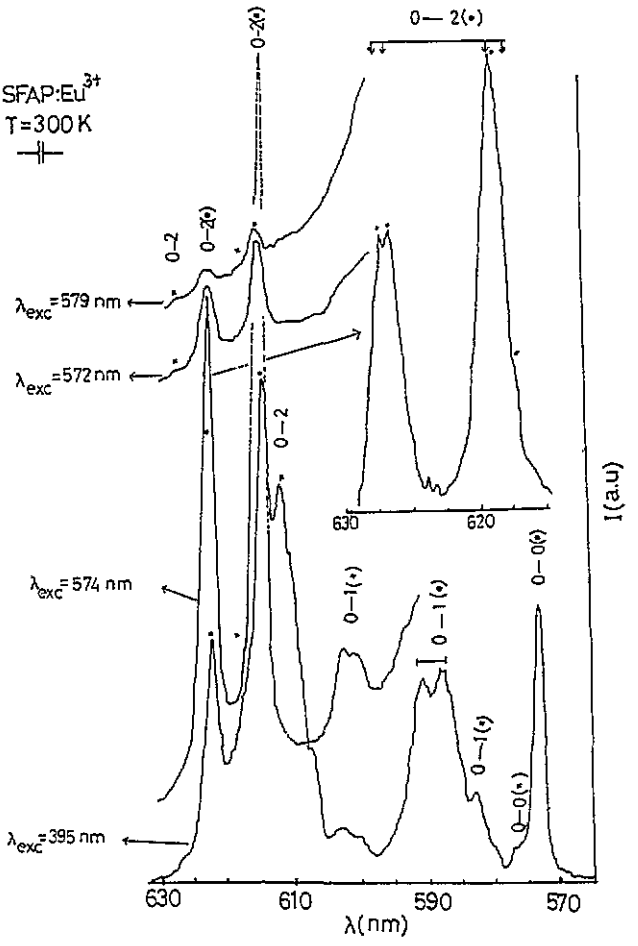

Figure 3. Eu^{3+} emission spectra for SFAP under different excitation conditions (a.u., arbitrary units): ●, emission components of the predominant $Eu^{3+}(M_{II})$ sites; ×, emission components of the less dominant $Eu^{3+}(M_I)$ sites; the inset shows the presence of four Stark components for the $^5D_0 \rightarrow {}^7F_2$ transition of the $Eu^{3+}(M_{II})$ centre. 0–0, 0–1 and 0–2, $^5D_0 \rightarrow {}^7F_J$ ($J = 0$, 1 and 2, respectively) transitions.

appear in the form of halogen (X^-) being replaced by oxygen. This can be expected from the well known example of Sb^{3+} luminescence in calcium halophosphate phosphor, wherein Sb^{3+} occupying the Ca_{II} site is charge compensated by O^{2-} in the F^-/Cl^- position [12]. The same mechanism of charge compensation should hold good in the present system too. However, the observation that the crystal-field splitting between different ^7F_J levels (table 2 and figure 2) and the profound dependence of the occurrence of $^5D_0 \rightarrow {}^7F_0$ emission on the type of X^- ion involved in apatites makes us conclude that X^- ions in the second type of cationic (M_{II}) sites remain intact. Alternatively, two $Ca^{2+}(M^{2+})$ ions being replaced by two Eu^{3+} with one additional oxygen should be possible, in which case Eu^{3+} should occur in pairs in either *cis* or *trans* geometries, resulting in two kinds of $Eu^{3+}(M_{II})$ as has been suggested by Priou *et al* [7]. However, we fail to observe any proof for the presence of two types of Eu^{3+} pairs in this system and it appears to us, for the moderate Eu^{3+} concentration used (5 mol%), pairing of Eu^{3+} ions be minimal. Hence, we suggest that

the charge-compensating species, namely free oxygen, should occur as an interstitial in the vicinity of the Eu^{3+} luminescent centre. It is reasonable to expect that the open channel (along the z axis) of the apatite should provide enough space to accommodate the interstitial oxygen atoms created during the process of charge compensation. Furthermore, the charge-compensating species should work in such a way that the Eu^{3+} luminescent centre is in an eight-coordinated system possessing tetragonal symmetry (for which the $^5D_0 \rightarrow {}^7F_2$ level will have four components) as is apparent from the observation that the high-energy Stark components at 16515 cm^{-1} and 16474 cm^{-1} (605.5 nm and 607 nm, respectively) fail to be resolved (indicated by an arrow in figure 2(a)) to account for the C_{1h} symmetry for which the entire J-fold degeneracy ought to have been lifted (for $J = 2$, ^7F_J will have five components). This is corroborated from the observation that some of the $^5D_0 \rightarrow {}^7F_J$ ($J = 0$, 1 and 2) emission lines, in particular the non-degenerate $^5D_0 \rightarrow {}^7F_0$ line at 576 nm, are inhomogenously broadened, indicating the distorted nature of the Eu^{3+} site.

On 572 nm excitation corresponding to the second $^5D_0 \rightarrow {}^7F_0$ level representing the other type of Eu^{3+} site in which Eu^{3+} occupies M_I sites of the apatite system [$Eu^{3+}(M_I)$], we observe a different type of emission pattern. In this case, for the $^5D_0 \rightarrow {}^7F_2$ emission, there are three new components at 15936 cm^{-1}, 15987 cm^{-1} and 16083 cm^{-1} (at 627.5 nm, 625.5 nm and 621.8 nm, respectively, in figure 2(a)) appearing in addition to the subdued $^7F_2$ components due to the $Eu^{3+}(M_{II})$ site. Fitting this into table 1 predicting the number of Stark components for different site symmetries indicates that trigonal symmetry is acting on Eu^{3+} centres occupying M_I sites. However, the Stark component at about 15898 cm^{-1} (at 629 nm) appeared diffuse and the weak emission lines at 16420 cm^{-1} and 16447 cm^{-1} (at 609 nm and 608 nm, respectively, indicated by an open circle in figure 2 and by an asterisk in table 2) point to the conclusion that in this system there may be some irregular sites as these are too weak to be attributed to Eu^{3+} occupying regular sites, namely M_I and M_{II}. Furthermore, in order to confirm the occupancy of various cationic sites by Eu^{3+}, the emission spectrum was recorded for the CFAP sample having the lowest Eu^{3+} concentration (0.5 mol%) in which the intersite energy transfer will be a minimum. On comparing the emission spectra of the samples having 0.5 and 5 mol% Eu^{3+} (figure 2(a), curves i and ii), the following observations can be made.

Table 1. Stark splitting pattern for different ^7F_J levels of Eu^{3+} under different site symmetries possible in $M_5(PO_4)_3X$ apatites.

Site symmetry	Splitting pattern (number of Stark components)		
	$J = 0$	$J = 1$	$J = 2$
$C_3(M_I)$	A (1)	A + E (2)	A + 2E (3)
$C_{1h}(M_{II})$	A (1)	3(A/B)	5(A/B)
$C_4(M_{II}$ modified)	A (1)	A + E (2)	A + 2B + E (4)

At low Eu^{3+} concentrations, there is no emission due to Eu^{3+} occupying M_I sites. Emission from Eu^{3+} in the M_{II} sites, and in particular the $^5D_0 \rightarrow {}^7F_2$ transition, appears with prominent features. Interestingly the corresponding $^5D_0 \rightarrow {}^7F_0$ emission is very weak compared with the sample having a higher Eu^{3+} concentration. One can also observe the emission features due to a third kind of site whose origin is not clear. However, we note that the $^5D_0 \rightarrow {}^7F_0$ and $^7F_1$ emission intensities are comparable with that of Eu^{3+} in regular sites, but the $^5D_0 \rightarrow {}^7F_2$ emission due to this site is too weak and diffuse to make any precise conclusion possible. Still, it seems reasonable to expect that this cannot

Table 2. Stark components of various $^5D_0 \rightarrow {}^7F_J$ ($J = 0$, 1 and 2) transitions of Eu^{3+} under different sites possible in the apatite host(s) ($T = 300$ K; Eu^{3+} concentration, 5 mol%). The asterisks (*) denote emission due to Eu^{3+} pairs or Eu^{3+} in irregular sites.

	Stark components (cm^{-1})		
Host	$J = 0$	$J = 1$	$J = 2$
CFAP, M_{II}	17361	17212, 17123, 16995	16515, 16474, 16247, 16048, 16012
CFAP, M_I	17483	17050, 16935, 16828	16083, 15987, 15936, 16447*, 16420*, 15898*
SFAP, M_{II}	17422	17028, 16909, 17169*	16181, 16155, 15962, 15949
SFAP, M_I	17271	16647, 16589	16453, 16337, 16205
CCAP	17513	17153, 16849	16393, 16353, 16260, 16077*
	17414		
	17316		
SCAP	17422	17051, 16935	16367, 16260, 16090*
	17331		
	17301		
CBAP	17483	16742, 16708	16129, 16103, 15987, 15962
	17331	16920	16502*, 16475*, 16366*, 15823*
CHAP	17331	17014, 16963	16380, 16300, 16287, 16247, 16234, 16221
	17271	16949, 16892, 16835	16116, 15987

arise from pairing of Eu^{3+} centres because these emission features occur even for low Eu^{3+} concentration. However, the inhomogenously broadened spectral features point to the conclusion that these may occur from distorted sites arising out of a different charge-compensating mechanism.

Hence, from the above observations we conclude for the CFAP system the following.

(i) Eu^{3+} ions preferentially occupy M_{II} sites rather than M_I sites.

(ii) Intersite energy transfer is not pronounced.

(iii) The presence of a third kind of Eu^{3+} site whose origin is not clear is equally probable.

Owing to the experimental limitations we have not attempted to study CFAPs further.

3.3.2. Strontium fluoroapatites: Eu^{3+}. The emission spectrum of Eu^{3+} in SFAP is shown in figure 3. For the non-selective excitation at 395 nm ($^7F_0 \rightarrow {}^5L_6$ transition of Eu^{3+}), the emission spectrum looks relatively simple compared with that of CFAP. On the basis of similar arguments given in the previous section, the intense line at 574 nm can be assigned to Eu^{3+} occupying M_{II} sites. For the selective excitation at this level (574 nm excitation), the numbers of Stark components for the $^5D_0 \rightarrow {}^7F_1$ and $^7F_2$ transitions are two and four, respectively, although the Stark splitting in the latter is not very pronounced (figure 3, inset). This enables us to conclude that Eu^{3+} in a Sr_{II} site works as though it is in an octacoordinated system having the local symmetry that can be described by a tetragonal system. This observation, in our opinion is different from the C_s point group symmetry reported by Zounani *et al* [8]. For selective excitation in the region 574–576 nm, one could see the absence of weak emission features that were present for the non-selective excitation. By fitting the number of Stark components that can be expected for C_3 symmetry (corresponding to M_I sites) it can be concluded that these weak features arise because Eu^{3+} occupies the second kind (namely M_I) of divalent cationic sites of the apatite system. In the excitation spectra (especially in the region 560–580 nm corresponding to the $^5D_0 \rightarrow {}^7F_0$

transition) used to monitor different $^5D_0 \rightarrow {}^7F_2$ components, we observe only one kind of $^5D_0 \rightarrow {}^7F_0$ line, and this line is slightly broadened when the emission is monitored at 612 nm (the dominant emission line corresponding to Eu^{3+} in M_{II} site). Comparing these results with those obtained for CFAP, the emission features of $Eu^{3+}(M_I)$ sites are interesting. In order to explain these weak inhomogenously broadened emission features the following two possibilities can be explored.

The transition probability for these transitions of Eu^{3+} occupying M_I sites can be low as the site symmetry might have changed because of the charge-compensating species; the geometry of the system should be closer to the centrosymmetric system in which case the electric dipole transition is expected to be forbidden. In our opinion this will have a minimum effect because the geometry of M_I remains intact as can be seen from the Stark splitting pattern and the results corresponding to its calcium analogue.

Alternatively, intense resonant transfer to $Eu^{3+}(M_{II})$ should be the active mechanism to account for the weak emission intensity. Furthermore it appears to us that the relative abundance of these sites should be low compared with the $Eu^{3+}(M_{II})$ site. This seems to be quite possible because the excitation spectrum used to monitor these lines leads to a similar pattern that is comparable to that of the former except that these are slightly broadened due to the distorted nature of the site.

Hence we conclude that Eu^{3+} in the SFAP system predominantly occupies M_{II} sites and the intense resonant transfer from $Eu^{3+}(M_I)$ to $Eu^{3+}(M_{II})$ makes the emission from M_I sites very weak.

3.4. Eu^{3+} luminescence in calcium and strontium chloroapatites

The emission spectra of Eu^{3+} in calcium chloroapatite (CCAP) and strontium chloroapatite (SCAP) are given in figure 4 and it can be seen that, except for the $^5D_0 \rightarrow {}^7F_0$ transition which has three components, the other transitions (higher J-values) are not sufficiently resolved to make a detailed study possible. However, from the observation that there are three components for the non-degenerate transition, the presence of three kinds of Eu^{3+} site is obvious. Unlike the fluoroapatites, all these transitions are very weak and equally intense, thus rendering selective excitation impossible. The absence of intense $^5D_0 \rightarrow {}^7F_0$ emission in this system is interesting and is discussed later (section 3.7).

3.5. Eu^{3+} luminescence in calcium hydroxyapatite

The emission spectra of Eu^{3+} in CHAP (in both the precipitated and calcined cases) are given in figure 5. It can be seen that the emission spectra are well resolved for calcined hydroxyapatite compared with those of precipitated hydroxyapatite. It is known from the x-ray powder patterns that the latter is x-ray amorphous and hence it is it is not surprising that Eu^{3+} emission in the precipitated hydroxyapatite is inhomogeneously broadened.

Now, in order to explain the Eu^{3+} emission in the calcined hydroxyapatite, we see that there are two weak $^5D_0 \rightarrow {}^7F_0$ lines (figure 5, inset), clearly indicating the presence of two types of Eu^{3+} site in this system. However, these lines are too weak to facilitate selective excitation. Also the Stark splitting between the different J manifolds of the $^5D_0 \rightarrow {}^7F_1$ and $^7F_2$ transitions is so small that it is difficult to assign the components to a particular site without ambiguity. For this reason we have not attempted to explain this further. However, we note that for the $^5D_0 \rightarrow {}^7F_1$ transition it is possible to estimate the Stark splitting between the two components, because the difference between the energies of the Stark components of both sites is almost negligible. In general the total number of Stark

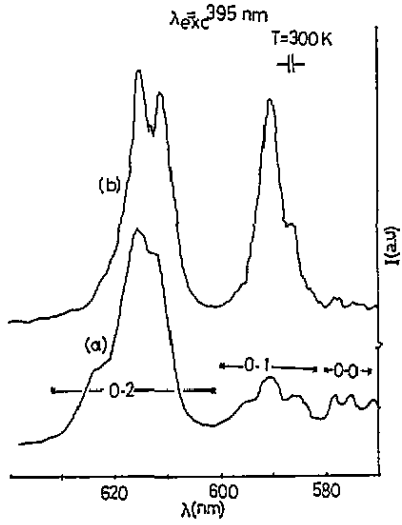

Figure 4. Eu^{3+} emission spectra for CCAP (curve (a)) and SCAP (curve (b)) (a.u., arbitrary units): 0–0, 0–1 and 0–2, emission components of $^5D_0 \rightarrow {}^7F_J$ (0, 1 and 2, respectively) transitions.

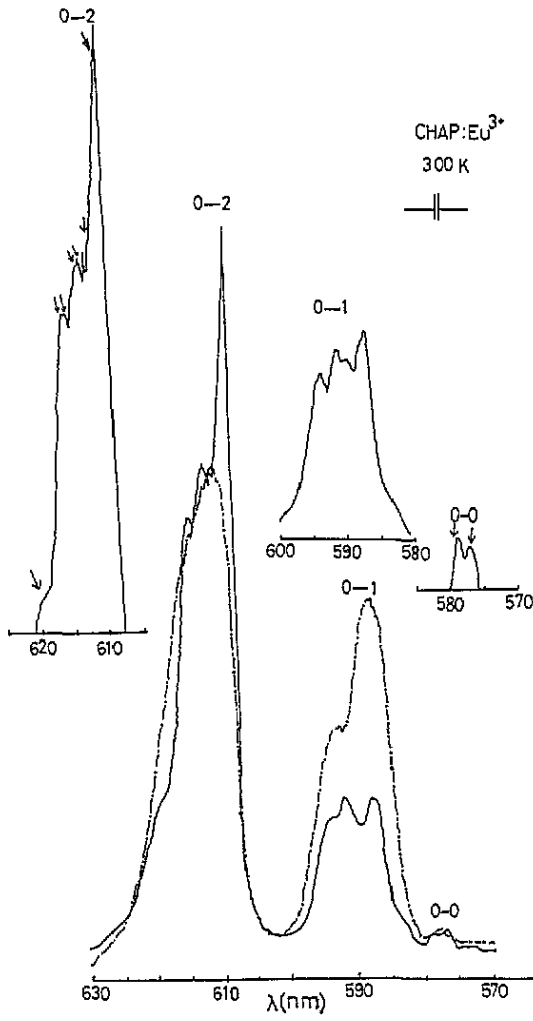

Figure 5. Emission spectra of Eu^{3+} for (a) precipitated, oven-dried (— · —) and (b) heat-treated samples (——) of CHAP: 0–0, 0–1 and 0–2 denote emission components of $^5D_0 \rightarrow {}^7F_J$ ($J = 0$, 1 and 2, respectively) transitions ($\lambda_{exc} = 395$ nm). The insets show resolved spectra of the different Stark components of various transitions of Eu^{3+}.

components observed for different $^5D_0 \rightarrow {}^7F_J$ ($J = 0, 1$ and 2) transitions are consistent with the total number of Stark components that can be expected under C_4 (modified C_2) + C_3 symmetries for which case $J = 0, 1$ and 2 and the Stark components are 2, 4 and 7, respectively. Another interesting feature of Eu^{3+} luminescence in hydroxyapatite is the absence of intense $^5D_0 \rightarrow {}^7F_0$ emission and this has been explained qualitatively in section 3.7.

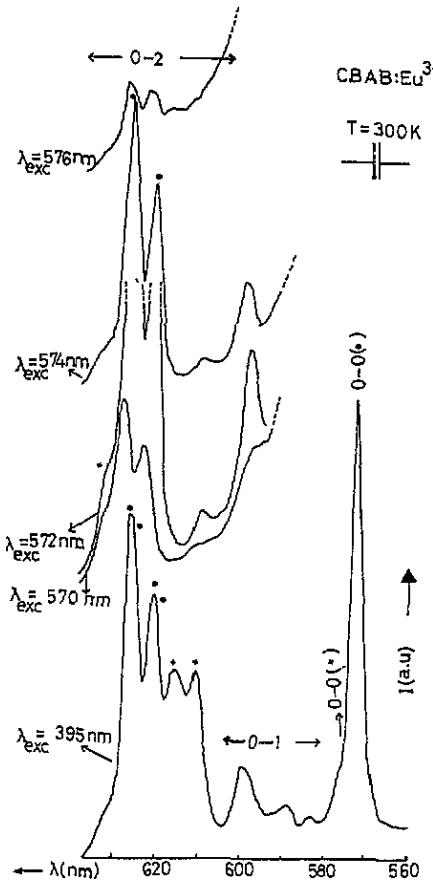

Figure 6. Emission spectrum of Eu^{3+} in CBAP: 0–0, 0–1 and 0–2, emission components of $^5D_0 \rightarrow {}^7F_J$ ($J = 0, 1$ and 2, respectively) transitions. The site assignments are the same as in figure 2.

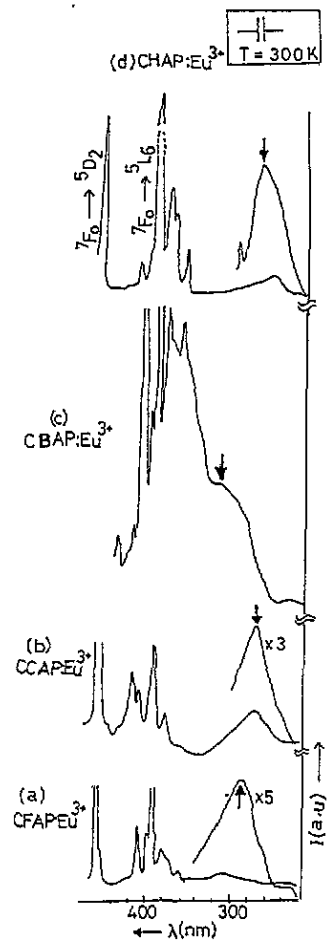

Figure 7. Excitation spectra used to monitor the dominant $^5D_0 \rightarrow {}^7F_2$ emission of Eu^{3+} (M_{II}) in various apatites (a.u., arbitrary units): from the bold arrows indicate the excitation maxima in various cases, the shift in CTB excitation band can be observed.

3.6. Eu^{3+} in calcium bromoapatite

The emission spectrum of Eu^{3+} in the calcium bromoapatite (CBAP) host is given in figure 6. From the spectrum and table 2, it can be seen that Eu^{3+} in this system occupies both types of site. In this system, consistent with our observations made earlier for the other apatite systems, the Stark splitting in Eu^{3+} (in M_{II} sites) levels works as though it is in tetragonal symmetry (i.e. for the $^5D_0 \rightarrow {}^7F_{0,1\&2}$ transitions there are one, two and four Stark components). However, the Stark splitting for the case of Eu^{3+} occupying the M_I site in this host is too small and the emission intensities are too weak to make a detailed study. Also, the weak emission intensity observed for the $^5D_0 \rightarrow {}^7F_0$ transition in this system is explained in section 3.7.

3.7. Crystal-field parameter B_{20} and $^5D_0 \rightarrow {}^7F_0$ emission

It is known that an ion placed in a crystalline medium experiences an electrostatic field that can be described by the Hamiltonian [13]

$$H = H_F + V_{CF} \tag{3}$$

where H_F is the free-ion Hamiltonian and V_{CF} is the crystal-field term that can be expressed as

$$V_{CF} = \sum_{kqi} B_{kq}(C_{kq})_i \tag{4}$$

where B_{kq} and C_{kq} are the crystal-field parameters and i extends over all the electrons involved. In this expression the second-rank crystal-field parameter B_{20} is very sensitive to the electrostatic interaction contributed by the surrounding ligands of the host matrix that can be given by the relation [14]

$$B_{20} \propto (3Z^2 - \gamma^2)/\gamma^3. \tag{5}$$

The second-rank crystal-field parameter B_{20} for Eu^{3+} in various apatites (for C_4 symmetry (modified sites)) can be calculated with knowledge of the crystal-field splitting between the two Stark components of the $^5D_0 \rightarrow {}^7F_1$ level. The $^5D_0 \rightarrow {}^7F_1$ magnetic dipole transition is of special importance in that its emission intensity is structure and symmetry independent and for this reason it can be used as internal standard in the estimation of transition probabilities for the other transitions of Eu^{3+}. The Stark components of the $^5D_0 \rightarrow {}^7F_1$ transition having structural invariance can be given by the relations [15]

$$H_{00} = -2\alpha_1 B_{20} \tag{6}$$

$$H_{11} = \alpha_1 B_{20} \tag{7}$$

where α_1 is the operator equivalent whose value can be obtained from the work of Lempicki *et al* [15]. Using this and the values of splitting between the Stark components of the $^5D_0 \rightarrow {}^7F_1$ transition, corresponding to the $Eu^{3+}(M_{II})$ sites of the various apatites, the value of the second-rank crystal-field parameter B_{20} can be calculated and the values for Eu^{3+} in different host lattices are given in table 3.

Table 3. Relative integrated (RI) emission intensities of $^5D_0 \rightarrow {}^7F_0$ and $^5D_0 \rightarrow {}^7F_2$ transitions with respect to the $^5D_0 \rightarrow {}^7F_1$ transition and crystal-field parameter B_{20} in various $M_5(PO_4)_3X$:Eu^{3+} (for M_{II} sites; T = 300 K).

Host	$\frac{RI(^5D_0 \rightarrow {}^7F_0)}{RI(^5D_0 \rightarrow {}^7F_1)}$	$\frac{RI(^5D_0 \rightarrow {}^7F_2)}{RI(^5D_0 \rightarrow {}^7F_1)}$	B_{20} (cm^{-1})
CFAP	1.5	3.5	362
SFAP	0.5	2.3	433
CCAP	0.05	3.5	240
SCAP	$\leqslant$0.01	2.0	193
CBAP	2.0	4.2	$\simeq$330
CHAP	0.02	2.1	$\simeq$250

Table 3 also gives the values of the relative intensities of $^5D_0 \rightarrow {}^7F_{0\&2}$ transitions with respect to the structure-independent $^5D_0 \rightarrow {}^7F_1$ transition. It can be seen that the magnitude of the relative intensity of the non-degenerate forbidden transition is about two orders higher for the fluoroapatites and bromoapatites than for the chloroapatites and hydroxyapatites.

Also the values of B_{20} for the fluoroapatites and bromoapatites are about twice those of the other two apatite systems.

It is pertinent to note that, as all these apatites are isomorphous in the broad sense of the term, they should have similar local site symmetries for the $Eu^{3+}(M_{II})$ sites, which should allow a linear field term in the expression for the crystal-field potential. This will facilitate the occurrence of the forbidden transition [16]. However, the observation that the occurrence of the forbidden transition has a profound dependence on the type of apatite ($X = F^-$, Cl^-; Br^- or OH^-) leads us to propose that this is not the case in the present investigation.

Alternatively, the higher B_{20}-values observed for the fluoroapatites and bromoapatites may lead to an admixture of higher J states with the forbidden $J = 0 \not\rightarrow 0$ transition. Hence this transition should occur through the process of J mixing rather than by the previous mechanism. Also it can be seen from the excitation spectra (figure 7) that there is a shift by about 4000–5000 cm^{-1} towards a lower energy in the Eu^{3+}–O^{2-}/X^- ($4f^7 2p^{-1}$) charge-transfer excitation band (CTB) for fluoroapatites and bromoapatites. This will lead to the admixture of an odd-parity septet state of the CTB with the $^7F_0$ state. This can also be an active mechanism for the occurrence of the intense forbidden transition [17].

4. Conclusions

Eu^{3+} in $M_5(PO_4)_3X$ apatites occupies both types of site, namely M_I and M_{II}, predominantly the latter. Also it has been found there exists a third kind of Eu^{3+} site whose origin is not clear. This can possibly arise out of a different charge-compensating mechanism other than proposed for $Eu^{3+}(M_{II})$ sites. We find that the site symmetry of the predominant $Eu^{3+}(M_{II})$ becomes modified so that it is closer to tetragonal symmetry owing to the charge-compensating species. Furthermore, the occurrence of intense $^5D_0 \rightarrow {}^7F_0$ emission of Eu^{3+} in some of the apatites can be attributed to J-mixing effects and admixture of odd-parity states.

Acknowledgments

Sincere thanks are due to Professor G V Subba Rao and Dr A S Lakshmanan of CECRI for their critical comments on the manuscript. Thanks are also due to the DST, New Delhi, for the award of a research grant (SP/S2/M-31/90). Also we thank the referees of this paper for pointing out the mistakes and for their valuable suggestions.

References

[1] Butler K H 1986 *Fluorescent Lamp Phosphors* (University Park, PA: Pennsylvania State University Press)
[2] Budin J P, Michel J C and Auzel F 1979 *J. Appl. Phys.* **50** 641
[3] Kaniya K, Tanahashi M, Suzuki T and Tanaka T 1990 *Mater. Res. Bull.* **25** 63
[4] Sudarsan K, Mackie T E and Young R A 1972 *Mater. Res. Bull.* **7** 1331
Mackie P E, Elliot J C and Young R A 1977 *Acta Crystallogr.* B **28** 1840
[5] Ropp R C 1991 *Studies in Inorganic Chemistry* vol 12 *Luminescence and the Solid State* (Amsterdam: Elsevier) ch 10
[6] Blasse G 1975 *J. Solid State Chem.* **14** 181 and references therein
[7] Priou B, Fahmi D, Dexpert-ghys J, Taitai A and Lacout J L 1987 *J. Lumin.* **39** 97
[8] Zounani A, Zambon D and Cousseins J C 1992 *J. Alloys Compounds* **188** 82
[9] Jagannathan R, Rao R P and Narayanan R L 1990 *ECS Extd Abstracts* **90–2** 646
Jagannathan R, Manoharan S P, Rao R P and Kutty T R N 1990 *Japan. J. Appl. Phys.* **29** 1991

[10] Blasse G 1979 *Handbook on the Physics and Chemistry of Rare Earths* eds K A Gschneidner Jr and L Eyring (Amsterdam: North-Holland) ch 34
[11] Tinkham M 1964 *Group Theory and Quantum Mechanics* (New York: McGraw-Hill)
[12] Ouweltjes J L 1951 *Philips. Tech. Rev.* **13** 346
[13] Wybourne B G 1965 *Spectroscopic Properties of Rare Earths* (New York: Interscience)
[14] Capobianco J A, Proulx P P, Bettinelli M and Negrisolo F 1990 *Phys. Rev.* B **42** 5936
[15] Lempicki A, Samelson H and Brecher C 1968 *J. Mol. Spectrosc.* **27** 375
[16] Nieuwpoort W C and Blasse G 1966 *Solid State Commun.* **4** 227
[17] Nishimura G, Tanaka M, Kurita A and Kushida T 1991 *J. Lumin.* **48–49** 473